# A Two-terminal Active Inductor with Minimum Apparent Power for the Auxiliary Circuit

Wang, Haoran; Wang, Huai

*Published in:*
I E E E Transactions on Power Electronics

*DOI (link to publication from Publisher):*
10.1109/TPEL.2018.2848668

*Publication date:*
2019

*Document Version*
Accepted author manuscript, peer reviewed version

This article has been accepted for publication in a future issue of this journal, but has not been fully edited. Content may change prior to final publication. Citation information: DOI 10.1109/TPEL.2018.2848668, IEEE Transactions on Power Electronics



# Letters

# A Two-terminal Active Inductor with Minimum Apparent Power for the Auxiliary Circuit

Haoran Wang, *Student Member*, *IEEE* and Huai Wang, *Senior Member*, *IEEE*

***Abstract*—This letter proposes a concept of a two-terminal active inductor with minimum apparent power processed by the auxiliary circuits, which are implemented by power semiconductor switches and passive elements. It has the same level of convenience as a passive inductor with two power terminals only. Compared with a conventional inductor with the same equivalent inductance and current rating, the energy storage requirement of the inductor can be reduced significantly, as well as the weight and volume. The auxiliary circuit in the active inductor processes both partial voltage and partial current, with the lowest apparent power rating compared to existing solutions. A case study for the DC-link filter inductor in a three-phase diode-bridge rectifier is discussed. Proof-of-concept experimental results are given to verify the functionality and effectiveness of the proposed active inductor.**

***Index Terms*—Active circuits, inductor, impedance element, power converter**

## I. Introduction

POWER semiconductor, capacitor and inductor are the basic elements in power electronic systems. Passive elements such as inductor and capacitor still have considerably lower power density compared to active switches [1]. Based on the duality of a two-terminal active capacitor concept proposed in [2], this letter proposes a two-terminal active inductor. It could achieve the same equivalent impedance characteristics of interest as a passive inductor while with a reduced inductive energy storage, implying the potential to size and weight reduction. Fig. 1 shows the duality between the two concepts. The proposed active inductor concept distinguishes itself from the ones discussed in [1] and [3–5] from two aspects: 1) it has two terminals only same as a conventional passive inductor without any external feedback signal and power supply, and 2) the auxiliary circuit in the proposed inductor processes the lowest apparent power, which is the theoretical minimum limit. The proposed active inductor can be controlled to have its impedance characteristics equivalent to a bulky passive inductor within a certain frequency range of interest.

Figs. 2 (a) and (b) show the concept of the existing active inductors and the proposed one, respectively. Terminals $A$ and $B$ are the ones that a passive inductor would be connected to a power electronic circuit. The current $i_{\mathrm{AB}}$ is an AC current or with DC bias, consisting of the main frequency component

The authors are with Center of Reliable Power Electronics (CORPE), the Department of Energy Technology, Aalborg University, 9220 Aalborg, Denmark (e-mail:hao@et.aau.dk and hwa@et.aau.dk).

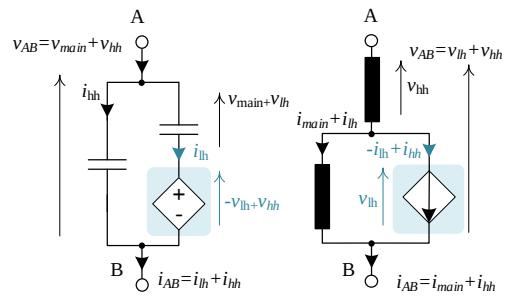


Minimum apparent power ≈ $V_{\mathrm{lh}} \times I_{\mathrm{lh}}$

(a) The active capacitor concept in [2].

(b) The proposed active inductor concept.

Fig. 1. The duality between the two-terminal active capacitor in [2] and the proposed active inductor concept. $v_{\mathrm{AB}}$, $i_{\mathrm{AB}}$ are the instantaneous terminals' voltage and current, respectively. $v_{\mathrm{main}}$, $v_{\mathrm{lh}}$ and $v_{\mathrm{hh}}$ are the instantaneous main voltage, low-frequency and high-frequency harmonic voltage, respectively. $i_{\mathrm{main}}$, $i_{\mathrm{lh}}$, and $i_{\mathrm{hh}}$ are the instantaneous main current, low-frequency and high-frequency harmonic current, respectively. $V_{\mathrm{lh}}$ and $I_{\mathrm{lh}}$ are the Root Mean Square (RMS) values of $v_{\mathrm{lh}}$ and $i_{\mathrm{lh}}$, respectively.

$i_{\mathrm{main}}$ and undesirable ripples, depending on specific applications. The auxiliary circuit (i.e., the controlled-voltage source) in Fig. 2 (a) generates a voltage that follows the undesirable voltage ripples of $v_{\mathrm{AB}}$, usually the low-frequency harmonics of interest (i.e., $v_{\mathrm{lh}}$). Therefore, the inductor $L_{\mathrm{f}}$ has high-frequency harmonics only if the auxiliary circuit operates ideally. It can be noted that the auxiliary circuit needs to process the entire current $i_{\mathrm{AB}}$, approximated as $i_{\mathrm{main}}$ if the high-frequency harmonics $i_{\mathrm{hh}}$ is ignored. Different from the concept shown in Fig. 2 (a), the proposed auxiliary circuit generates a controlled-current source as shown in Fig. 2 (b) and processes a partial current only. Moreover, none of the methods presented in [1] and [3–5] can implement a plug-and-play active inductor since they have more terminals, such as external feedback signals and auxiliary power supplies for the controller and gate drivers. This letter presents the concept of the proposed active inductor and one of the implementations by applying the self-power method presented in [2] and a current control strategy without external feedback signal.

## II. The Concept and an Implementation of the Two-terminal Active Inductor

### A. Concept of the Two-terminal Active Inductor

As shown in Fig. 2 (b), the proposed active inductor consists of a high-frequency inductor $L_{\mathrm{f}}$, a low-frequency inductor $L_1$,

This article has been accepted for publication in a future issue of this journal, but has not been fully edited. Content may change prior to final publication. Citation information: DOI 10.1109/TPEL.2018.2848668, IEEE Transactions on Power Electronics



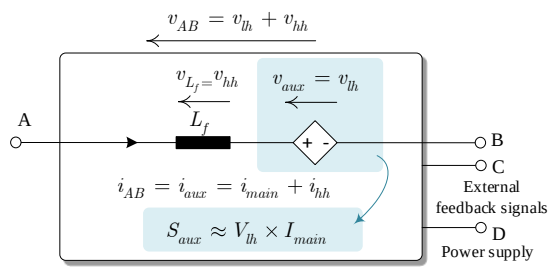


(a) The equivalent diagram of the active inductors proposed in [3-5].

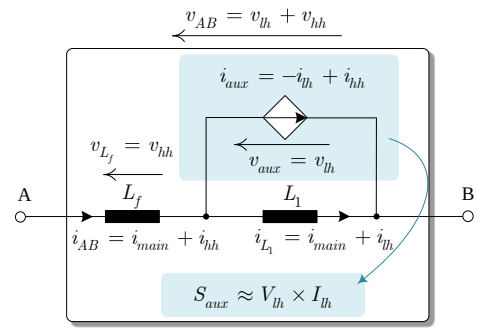


(b) The equivalent diagram of the proposed two-terminal active inductor.

Fig. 2. The equivalent diagrams of (a) existing active inductors and (b) the proposed two-terminal active inductor. $v_{\mathrm{AB}}$, $i_{\mathrm{AB}}$, $v_{\mathrm{aux}}$ and $i_{\mathrm{aux}}$ are the instantaneous voltage and current of the terminals and the auxiliary circuit, respectively. $v_{\mathrm{lh}}$ and $v_{\mathrm{hh}}$ are the instantaneous low-frequency and high-frequency harmonic voltage, respectively. $i_{\mathrm{main}}$, $i_{\mathrm{lh}}$, and $i_{\mathrm{hh}}$ are the instantaneous main current, low-frequency harmonic current and high-frequency harmonic current, respectively. $V_{\mathrm{lh}}$, $I_{\mathrm{lh}}$ and $I_{\mathrm{main}}$ are RMS values of low-frequency voltage, low-frequency current and main current, respectively. $S_{\mathrm{aux}}$ is the apparent power of the auxiliary circuit.

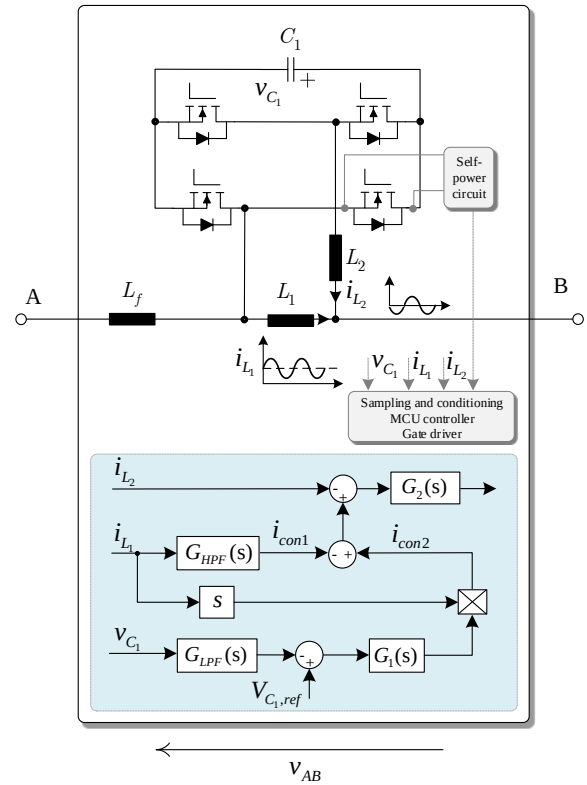


Fig. 3. An implementation of the proposed two-terminal active inductor with a current control strategy.

and a controlled-current source connected in parallel with $L_1$. The controlled-current source $i_{\mathrm{aux}}$ is equal to the undesirable low-frequency current harmonics $i_{\mathrm{lh}}$ of $L_1$ with out of phase and high-frequency harmonics $i_{\mathrm{hh}}$. The voltage across the controlled-current source is equal to the undesirable low-frequency voltage harmonics of $v_{\mathrm{aux}}$. Therefore, the auxiliary circuit used to implement the controlled-current source processes the partial voltage of $v_{\mathrm{AB}}$ and the partial current of $i_{\mathrm{AB}}$ only, as indicated in Fig. 2 (b).

A current control strategy is proposed for the auxiliary circuit which will be discussed specifically in Part B of Section II. It is based on internal voltage and current information of the auxiliary circuit. A self-power method implemented in [2] is applied for this study, which obtains the power for the digital controller and gate drivers from the active power switches in the auxiliary circuit. Therefore, the proposed concepts eliminate the use of external feedback signal and auxiliary power supply. The active inductor has two power terminals $A$ and $B$ only, making it as convenient as a conventional inductor.

### *B. An Implementation of the Two-terminal Active Inductor Concept*

One of the possible implementations of the proposed active inductor concept is shown in Fig. 3. A full-bridge bi-directional converter is used as the auxiliary circuit. $C_1$ is the DC-link capacitor of the auxiliary circuit and $L_2$ is the smoothing inductor. A self-power unit is used to obtain the power for gate drivers and controller in the active circuit from the drain-source terminals of a MOSFET, which can be referred to [2]. The objective is to control $i_{\mathrm{L_2}}$ to be out of phase with the harmonic component in $i_{\mathrm{L_1}}$ and with the same amplitude. The reference of $i_{\mathrm{L_2}}$ contains two parts: 1) $i_{\mathrm{con1}}$ is the extracted harmonic component of $i_{\mathrm{L_1}}$ which is used to modulate the converter to generate the desired $i_{\mathrm{L_2}}$; 2) $i_{\mathrm{con2}}$ is used to stabilize $v_{\mathrm{C_1}}$. The phase of $i_{\mathrm{con2}}$ and $i_{\mathrm{con1}}$ is synchronized (i.e., 90° phase shift with $i_{\mathrm{con1}}$), in order to absorb active power from external circuits through terminals $A$ and $B$ to compensate the power loss of the auxiliary circuit. Based on small-signal analysis [6], the impedance of the active inductor is obtained as

$$Z_{\mathrm{AB}} = \frac{\Delta v_{\mathrm{AB}}(s)}{\Delta i_{\mathrm{AB}}(s)} = \frac{\Delta i_{\mathrm{L_1}}(s) L_1 s}{\Delta i_{\mathrm{L_1}}(s) + \Delta i_{\mathrm{L_1}}(s) G_{\mathrm{r}}(s)} = \frac{L_1 s}{1 + G_{\mathrm{r}}(s)} \quad (1)$$

where $\Delta v_{\mathrm{AB}}(s)$, $\Delta i_{\mathrm{AB}}(s)$, $\Delta i_{\mathrm{L_1}}(s)$ and $\Delta i_{\mathrm{L_2}}(s)$ are the AC perturbations. $G_{\mathrm{r}}(s)$ is the transfer function from $\Delta i_{\mathrm{L_1}}(s)$ to $\Delta i_{\mathrm{L_2}}(s)$ as presented by (2). $M$ is the modulation index. $I_{\mathrm{L_2}}$ and $V_{\mathrm{C_1}}$ are the Root Mean Square (RMS) values of the inductor current $i_{\mathrm{L_2}}$ and capacitor voltage $v_{\mathrm{C_1}}$, respectively. $G_{\mathrm{HPF}}(\mathrm{s})$ and $G_{\mathrm{LPF}}(\mathrm{s})$ are the high pass filter (HPF) and low pass filter (LPF) in the conditioning circuits of $i_{\mathrm{L_1}}$ and $v_{\mathrm{C_1}}$, respectively. $G_1(\mathrm{s})$ and $G_2(\mathrm{s})$ are the PID controllers of the power loss compensation loop and current control loop, respectively.

## III. Application of the Active Inductor in a Three-phase Diode-bridge Rectifier

### *A. Component Sizing*

The specification of the case study is shown in Table I.

This article has been accepted for publication in a future issue of this journal, but has not been fully edited. Content may change prior to final publication. Citation information: DOI 10.1109/TPEL.2018.2848668, IEEE Transactions on Power Electronics



$$G_{\mathrm{r}}(s)=\frac{\Delta i_{\mathrm{L_2}}(s)}{\Delta i_{\mathrm{L_1}}(s)}=\frac{C_1L_1s^2+G_1(s)G_{\mathrm{LPF}}(s)G_2(s)L_1I_{\mathrm{L_2}}s-C_1G_{\mathrm{HPF}}(s)G_2(s)V_{\mathrm{C_1}}s+MG_{\mathrm{HPF}}(s)G_2(s)I_{\mathrm{L_2}}}{C_1L_2s^2+G_1(s)G_{\mathrm{LPF}}(s)G_2(s)L_2I_{\mathrm{L_2}}s+C_1G_2(s)V_{\mathrm{C_1}}s+M^2+MG_1(s)G_{\mathrm{LPF}}(s)G_2(s)V_{\mathrm{C_1}}-MG_2(s)I_{\mathrm{L_2}}} \tag{2}$$

TABLE I
SPECIFICATION OF A 900 W THREE-PHASE DIODE-BRIDGE RECTIFIER WITH A TWO-TERMINAL ACTIVE INDUCTOR.

| Parameters | Description |
|---|---|
| Three-phase diode-bridge rectifier | |
| P | Power rating, 900 W |
| $v_{\mathrm{AC}}$ | AC voltage (RMS), 110 V |
| $f_{\mathrm{a}}$ | Fundamental frequency, 50 Hz |
| $I_{\mathrm{main}}$ | Main component current, 3.8 A |
| $V_{\mathrm{DC-link}}$ | DC-link voltage, 240 V |
| Two-terminal active inductor | |
| $C_1$ | $C_1$, 470 $\mu$F/ 35 V NCC EKY-350ELL471MJ20S |
| $L_1$ | DC inductor $L_1$, 8 $m$H/ 6 A |
| $L_2$ | AC inductor $L_2$, 100 $\mu$H/ 2 A |
| $L_{\mathrm{f}}$ | AC inductor $L_{\mathrm{f}}$, 100 $\mu$H/ 6 A |
| $\alpha$ | Current ripple ratio of DC-link current, 17 % |
| $\beta$ | Current ripple ratio of $L_1$, 60 % |

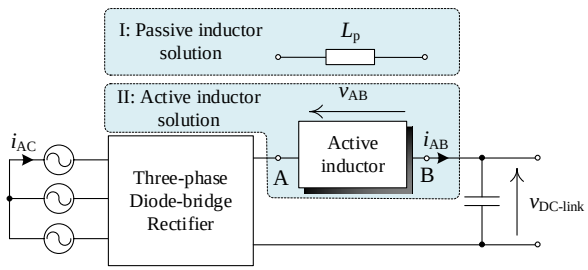


Fig. 4. System diagram of the three-phase diode-bridge rectifier with passive or active inductor solution.

The diagram of the three-phase diode-bridge rectifier with a two-terminal active inductor is shown in Fig. 4. The high-frequency current harmonics and high-frequency filter $L_{\mathrm{f}}$ are not considered in the following discussions. The inductance of $L_1$ is

$$L_1=\frac{2\sqrt{2}V_{\mathrm{lh}}}{\omega_{\mathrm{lh}}\beta I_{\mathrm{main}}} \tag{3}$$

where $V_{\mathrm{lh}}$ is the RMS value of low-frequency voltage harmonic of interest. $\omega_{\mathrm{lh}}$ is the angular frequency of the low-frequency harmonic. $\beta$ is the ripple current ratio of $L_1$. $\beta=\frac{I_{\mathrm{L_1-pp}}}{I_{\mathrm{main}}}$, where $I_{\mathrm{L_1-pp}}$ is the peak-to-peak value of the ripple current of $L_1$. Therefore, the value of $\beta$ determines the processed current in the auxiliary circuit. There is a trade-off between its apparent power and the inductance value $L_1$. In practice, there are high-frequency current harmonics in $i_{\mathrm{aux}}$ due to the non-ideal operation of the auxiliary circuit. The high-frequency current level depends on the values of $C_1$, $L_2$, and the switching frequency of the auxiliary circuit, which is not discussed here for the sake of simplicity. With the conventional inductor solution, the required inductance $L_{\mathrm{p}}$ is

$$L_{\mathrm{p}}=\frac{2\sqrt{2}V_{\mathrm{lh}}}{\omega_{\mathrm{lh}}\alpha I_{\mathrm{main}}} \tag{4}$$

where $\alpha$ is the ripple current ratio limit of $i_{\mathrm{AB}}$ (i.e., the DC-link current in the case study). The apparent power ratio between the auxiliary circuit of the proposed active inductor

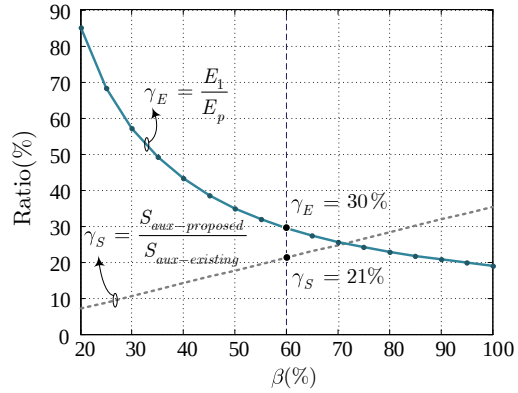


Fig. 5. Relation between ripple current ratio $\beta$ of $L_1$, apparent power ratio $\gamma_{\mathrm{S}}$ and energy storage ratio $\gamma_{\mathrm{E}}$ with 17 % current ripple ratio $\alpha$.

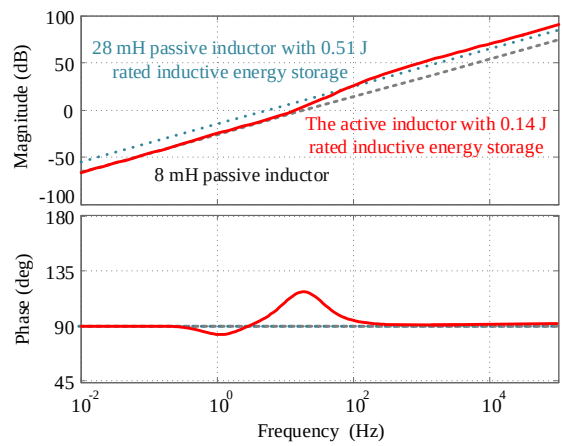


Fig. 6. Impedance curves of an active inductor with 0.14 J rated inductive energy storage and a passive inductor with 0.51 J rated energy storage.

in Fig. 2 (b) and the one of existing solutions in Fig. 2 (a) is

$$\gamma_{\mathrm{S}}=\frac{S_{\mathrm{aux-proposed}}}{S_{\mathrm{aux-existing}}}=\frac{V_{\mathrm{lh}}\times\frac{\beta}{2\sqrt{2}}I_{\mathrm{main}}}{V_{\mathrm{lh}}\times I_{\mathrm{main}}}=\frac{1}{2\sqrt{2}}\beta. \tag{5}$$

The actual energy storage ratio between $L_1$ of the active inductor and $L_{\mathrm{p}}$ of the passive solution is

$$\gamma_{\mathrm{E}}=\frac{E_1}{E_{\mathrm{p}}}=\frac{\frac{1}{2}L_1\left(\sqrt{I_{\mathrm{main}}^2+\left(\frac{\beta}{2\sqrt{2}}I_{\mathrm{main}}\right)^2}\right)^2}{\frac{1}{2}L_{\mathrm{p}}\left(\sqrt{I_{\mathrm{main}}^2+\left(\frac{\alpha}{2\sqrt{2}}I_{\mathrm{main}}\right)^2}\right)^2}=\frac{\alpha(8+\beta^2)}{\beta(8+\alpha^2)}. \tag{6}$$

In Fig. 5, $\alpha=17\%$ is selected as a case to investigate the relation between $\beta$, $\gamma_{\mathrm{S}}$ and $\gamma_{\mathrm{E}}$. With $\beta=60\%$, $L_{\mathrm{p}}=27.9$ mH, $L_1=7.9$ mH, $\gamma_{\mathrm{E}}=30\%$, and $\gamma_{\mathrm{S}}=21\%$. Considering the design margin, the passive components used in experimental setup are $L_{\mathrm{p}}=28$ mH/ 6 A with 0.51 J rated energy storage, $L_1=8$ mH/ 6 A with 0.14 J rated energy storage. Fig. 6 shows the impedance curve of the active inductor based on

This article has been accepted for publication in a future issue of this journal, but has not been fully edited. Content may change prior to final publication. Citation information: DOI 10.1109/TPEL.2018.2848668, IEEE Transactions on Power Electronics



the following parameters: $M = 0.9$, $I_{\mathrm{L}_2} = 0.9$ A, $V_{\mathrm{C}_1} = 25$ V, $\omega_{\mathrm{lh}} = 1884$ rad/sec, $G_{\mathrm{HPF}}(s) = 0.02s/(0.02s + 1)$ and $G_{\mathrm{LPF}}(s) = 1/(0.1s + 1)$, $G_1(s) = (0.1s + 2)/s$ and $G_2(s) = (0.005s^2+0.8s+10)/s$. In the frequency range below 50 Hz, the impedance characteristics of the active inductor is equivalent to a 8 mH inductor, which is determined by $L_1$. For a frequency at 100 Hz or above, the impedance of the active inductor is slightly higher than a 28 mH passive inductor. It implies that the active inductor can achieve a comparable equivalent inductance with 27.5 % rated inductive energy storage in the presented case study.

### B. Experimental Results

Fig. 7 shows the experimental waveforms of the diode-bridge rectifier with the implemented two-terminal active inductor with 0.14 J rated inductive energy storage. The power loss of the active inductor is 4 W in the presented case study, which is 0.44 % with respect to the apparent power of the main system. Fig. 7 (a) shows a 18 % current ripple of the DC link, with the peak-to-peak value of 0.7 A, which is slightly higher than the theoretical analysis due to the existence of high-frequency ripple current harmonics. Fig. 7 (b) shows the comparative results of the rectifier with a passive inductor with 0.51 J rated energy storage. The difference in the DC-link current ripple is negligible. The apparent power handled by the auxiliary circuit is 21 % of that in existing solutions shown in Fig. 2 (a). Fig. 8 presents the key waveforms of the active inductor. It can be noted that the ripple current of $i_{\mathrm{L}_1}$ is approximately out of phase with $i_{\mathrm{L}_2}$. The high-frequency current harmonics in $i_{\mathrm{L}_2}$ is due to the non-ideal operation of the auxiliary circuit, which appears at the DC-link current $i_{\mathrm{AB}}$. The slight phase shift is due to the absorbed active power for the power loss compensation of the auxiliary circuit. With a comparative analysis, the cost, volume and weight of the active inductor is 80.6 %, 68.6 % and 70.7 % of the passive inductor $L_{\mathrm{p}}$. The reliability comparison is still an open question. It could be a challenge in achieving the same level reliability performance, due to the fact that magnetic components are relatively more reliable than active switching devices and capacitors. Nevertheless, it is not necessarily an issue for practical applications due to the added auxiliary circuit is nothing special compared to a typical full-bridge inverter, which could fulfill the reliability requirement for majority of the industry applications through a proper design.

## IV. Conclusion

This paper proposes a two-terminal active inductor concept with a minimum apparent power for the auxiliary circuit. It enables a plug-and-play solution without any additional efforts compared to a conventional passive inductor. A current control strategy is applied based on internal feedback signals from the auxiliary circuit only. The key component parameters, energy storage, and the apparent power of the auxiliary active circuit are analyzed. In the case study, the implemented active inductor achieves almost an equivalent impedance curve to a 28 mH passive inductor at the frequencies of interest, while with 27.5% rated inductive energy storage and 21% apparent power compared to the existing solutions shown in Fig. 2 (a).

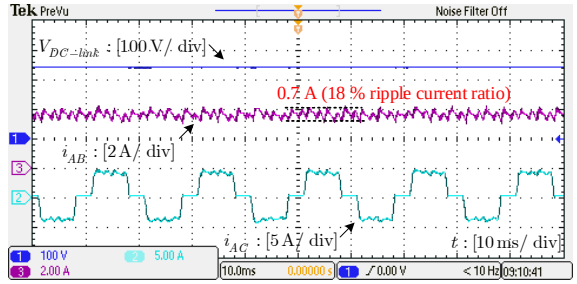


(a) Diode- bridge rectifier with an active inductor with 0.14 J rated inductive energy storage.

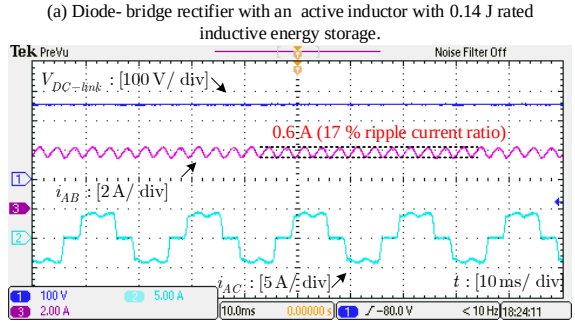


(b) Diode-bridge rectifier with a passive inductor with 0.51 J rated inductive energy storage.

Fig. 7. Experimental waveforms with the passive inductor and the active inductor in the DC link of the three-phase diode-bridge rectifier.

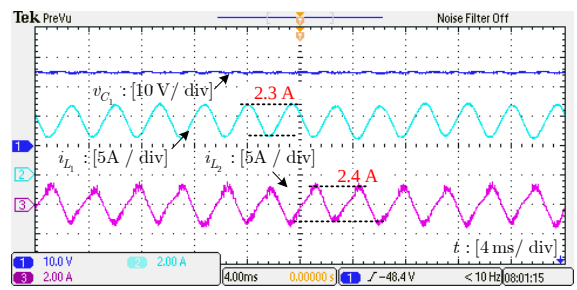


Fig. 8. Experimental waveforms of the active inductor in the case study.

## References

[1] H. Funato and A. Kawamura, "Proposal of variable active-passive reactance," in *Proc. International Conference on Industrial Electronics, Control, Instrumentation, and Automation*, 1992, pp. 381–388.

[2] H. Wang and H. Wang, "A two-terminal active capacitor," *IEEE Trans. on Power Electron.*, vol. 32, no. 8, pp. 5893–5896, Aug. 2017.

[3] S. Li, W. Qi, S. C. Tan, S. Y. R. Hui, and C. Tse, "A general approach to programmable and reconfigurable emulation of power impedances," *IEEE Trans. Power Electron.*, vol. 33, no. 1, pp. 259–271, Jan 2018.

[4] P. Davari, Y. Yang, F. Zare, and F. Blaabjerg, "A review of electronic inductor technique for power factor correction in three-phase adjustable speed drives," in *Proc. IEEE ECCE*, 2016, pp. 1–8.

[5] H. Ertl and J. W. Kolar, "A constant output current three-phase diode bridge rectifier employing a novel "electronic smoothing inductor"," *IEEE Trans. on Ind. Electron.*, vol. 52, no. 2, pp. 454–461, Apr. 2005.

[6] W. Liu, K. Wang, H. S. h. Chung, and S. T. h. Chuang, "Modeling and design of series voltage compensator for reduction of dc-link capacitance in grid-tie solar inverter," *IEEE Trans. Power Electron.*, vol. 30, no. 5, pp. 2534–2548, May 2015.